Vanadium(IV) Complexes with Mixed O,S Donor Ligands. Syntheses, Structures, and Properties of the Anions Tris(2-mercapto-4-methylphenolato)vanadate(IV) and Bis(2-mercaptophenolato)oxovanadate(IV)

Paul R. Klich,[1] Andrew T. Daniher,[2] and Paul R. Challen*,[3]

Department of Chemistry, John Carroll University, Cleveland, Ohio 44118

David B. McConville and Wiley J. Youngs

Department of Chemistry, University of Akron, Akron, Ohio 44325

Received June 26, 1995[⊗]

Reaction of $VO(acac)_2$ with 2-mercaptophenol (mpH_2) in the presence of triethylamine gives the mononuclear tris complex $(Et_3NH)_2[V(mp)_3]$ (**1**), in which the vanadyl oxygen has been displaced. An analogous reaction using 2-mercapto-4-methylphenol ($mmpH_2$) afforded $(Et_3NH)(PNP)[V(mmp)_3]$ (**2**), which was structurally characterized. **2** crystallizes in the orthorhombic space group $Pna2_1$ with unit cell parameters (at −163 °C) a = 23.974(7) Å, b = 9.569(4) Å, c = 25.101(6) Å, and Z = 4. The coordination geometry around the vanadium is between octahedral and trigonal prismatic. Reaction of $VO(acac)_2$ with the sodium salt of 2-mercaptophenol produces the vanadyl(IV) complex $Na(Ph_4P)[VO(mp)_2]\cdot Et_2O$ (**3**), which crystallizes in the triclinic space group $P\bar{1}$ with unit cell parameters (at −135 °C) a = 12.185(4) Å, b = 12.658(4) Å, c = 14.244(4) Å, α = 103.19(2)°, β = 100.84(2)°, and γ = 114.17(2)°. The unit cell of **3** contains a pair of symmetry-related $[VO(mp)_2]^{2-}$ units bridged through vanadyl and ligand oxygen atoms by a pair of sodium ions, in addition to two PPh_4^+ ions. The coordination geometry around the vanadium is square pyramidal, with a V═O bond length of 1.611(5) Å. **1**, **2**, and **3** are characterized by IR and UV−vis spectroscopies, magnetic susceptibility, EPR spectroscopy, and cyclic voltammetry. **1** and **2** can be oxidized by I_2, Cp_2Fe^+, or O_2 to $[V(mp)_3]^-$ and $[V(mmp)_3]^-$, respectively, which in turn can be reduced back to the dianions by oxalate ion. These reversible redox processes can be followed by UV−vis spectroscopy.

Introduction

The chemistry of vanadium in its higher oxidation states (III, IV, V) is dominated by halide, O, and N donors.[4] There is, however, a smaller but expanding set of vanadium(III,IV,V) complexes with ligands containing sulfur donors, of both the organometallic[5] and nonorganometallic[6] variety. Some of the impetus for research in this area has come from the recently discovered roles of vanadium in biological systems,[7] including the vanadium nitrogenase[8] in which sulfur donors form part of the coordination sphere. Further motivation has derived from the need to better understand the action of vanadium species in crude oil in poisoning hydrodesulfurization catalysts; the active poisons are V/S compounds derived from oxovanadium(IV) precursors with S, N, and/or O donors as ancillary ligands.[9] The processes by which S displaces O and N donors from vanadium(IV) are not completely understood. In addition, complexes of vanadium with dithiolene ligands (SCR═RCS) have recently been investigated as potential molecular conductors, as well as for their interesting crystallographic and electronic properties.[10]

Complexes of vanadium with ligands that provide a mix of O and S donors are rare. Oxovanadium(IV) mercaptocarboxylates have been investigated in aqueous solution,[11] while bis-

⊗ Abstract published in *Advance ACS Abstracts,* December 15, 1995.

(1) Present address: Geon Company, Cleveland, OH.

(2) Present address: Department of Chemistry, Washington University, St. Louis, MO.

(3) Author to whom correspondence should be addressed.

(4) Some recent articles: (a) Vergopoulos, V.; Jantzen, S.; Rodewald, D.; Rehder, D. *J. Chem. Soc., Chem. Commun.* **1995**, *3*, 377−378. (b) Shaver, A.; Hall, D. A.; Ng, J. B.; Lebuis, A.-M.; Hynes, R. C.; Posner, B. I. *Inorg. Chim. Acta* **1995**, *229*, 253−260. (c) Khan, M. I.; Haushalter, R. C.; O'Connor, C. J.; Tao, C.; Zubieta, J. *Chem. Mater.* **1995**, *7*, 593−595. (d) Wang, X.; Zhang, X. M.; Liu, H. X. *Polyhedron* **1995**, *14*, 293−296. (e) Bonadies, J. A.; Butler, W. M.; Pecoraro, V. L.; Carrano, C. J. *Inorg. Chem.* **1987**, *26*, 1218.

(5) (a) Zeltner, S.; Dietzsch, W.; Olk, R.-M.; Kirmse, R.; Richter, R. *Z. Anorg. Allg. Chem.* **1994**, *620*, 1768−1776. (b) Stephan, D. W. *Inorg. Chem.* **1992**, *31*, 4218−4223. (c) Herberhold, M.; Kuhnlein, M.; Kremnitz, W.; Rheingold, A. L. *J. Organomet. Chem.* **1990**, *383*, 71−84. (d) Duraj, S. A.; Andras, M. T.; Rihter, B. *Polyhedron* **1989**, *8*, 2763−2767. (e) Floriani, C.; Gambarotta, S.; Chiesi-Villa, A.; Guastini, C. *J. Chem. Soc., Dalton Trans.* **1987**, 2099−2103. (f) Bolinger, C. M.; Darkwa, J.; Gammie, G.; Gammon, S. D.; Lyding, J. W.; Rauchfuss, T. B.; Wilson, S. R. *Organometallics* **1986**, *5*, 2386−2388.

(6) (a) Dean, N. S.; Bartley, S. L.; Streib, W. E.; Lobkovsky, E. B.; Christou, G. *Inorg. Chem.* **1995**, *34*, 1608−1616. (b) Tsagkalidis, W.; Rodewald, D.; Rehder, D. *J. Chem. Soc., Chem. Commun.* **1995**, *2*, 165−166. (c) Tsagkalidis, W.; Rodewald, W.; Rehder, D. *Inorg. Chem.* **1995**, *34*, 1943−1945. (d) Kawaguchi, H.; Tatsumi, K.; Nakamura, A. *J. Chem. Soc., Chem. Commun.* **1995**, *1*, 111−112. (e) Wei, C.; MacDonnell, F. M.; Scott, M. J.; Holm, R. H. *Inorg. Chem.* **1994**, *33*, 5809−5818. (f) Money, J. K.; Huffman, J. C.; Christou, G. *Inorg. Chem.* **1988**, *27*, 507−514. (g) Halbert, T. R.; Hutchings, L. L.; Rhodes, R.; Stiefel, E. I. *J. Am. Chem. Soc.* **1986**, *108*, 6437−6438. (h) Attanasio, D.; Bellitto, C.; Flamini, A. *Inorg. Chem.* **1980**, *19*, 3419−3424.

(7) Rehder, D. *Angew. Chem., Int. Ed. Engl.* **1991**, *30*, 148.

(8) Hales, B. J.; Case, E. E.; Morningstar, J. E.; Dzeda, M. F.; Mauterer, L. A. *Biochemistry* **1986**, *25*, 7251.

(9) See references within ref 6a.

(10) (a) Livage, C.; Fourmigué, M.; Batail, P.; Canadell, E.; Coulon, C. *Bull. Soc. Chim. Fr.* **1993**, *130*, 761−771. (b) Martin, J. D.; Canadell, E.; Batail, P. *Inorg. Chem.* **1992**, *31*, 3176−3178. (c) Akiba, K.; Matsubayashi, G.; Tanaka, T. *Inorg. Chim. Acta* **1989**, *165*, 245−248. (d) Broderick, W. E.; McGhee, E. M.; Godfrey, M. R.; Hoffman, B. M.; Ibers, J. A. *Inorg. Chem.* **1989**, *28*, 2902−2904.

(11) Kiss, T.; Buglyo, P.; Micera, G.; Dessi, A.; Sanna, D. *J. Chem. Soc., Dalton Trans.* **1993**, *12*, 1849−1855.

0020-1669/96/1335-0347$12.00/0

(2-mercaptopyridine *N*-oxide)oxovanadium(IV) has recently been structurally characterized.[12] Kang et al. reported[13] the trinuclear non-oxo vanadium(IV) complex, $[V_3(mp)_6]^-$, and recently[14] the dimeric complex $[V(mp)_3NaLL']_2^{2-}$. These latter complexes contain the ligand 2-mercaptophenolate (mp^{2-}, $C_6H_4OS^{2-}$), which is related to the dithiolenes (e.g. $C_6H_4S_2^{2-}$) and to the catecholates (e.g. $C_6H_4O_2^{2-}$). Transition metal dithiolene complexes have received much attention over the past 30 years.[15] They display delocalized electronic structures and multiple reversible redox couples and were among the first six-coordinate complexes found to exhibit trigonal prismatic geometries. Likewise, the transition metal catecholates have been extensively studied over the past 20 years for their unique structural, magnetic, and electronic properties, and their chemistry has been recently reviewed.[16] The catecholate ligand can coordinate in its fully reduced form or as partially oxidized semiquinone or fully oxidized quinone forms, but the coordinated ligand is charge-localized. As with the dithiolenes, there may be ambiguity as to the oxidation state of the metal. The coordination geometry of the six-coordinate complexes is usually octahedral or distorted octahedral, but is sometimes trigonal prismatic.[17] Vanadium catecholates have found use as spectrophotometric analytical reagents,[18] have relevance to the bioinorganic chemistry of tunicates,[19] are active as catalysts in dinitrogen reduction,[20] and are intermediates in catechol oxidations.[21] While dithiolenes (and sulfur ligands in general) are soft Lewis bases and tend to stabilize metals in lower oxidation states, catecholates are hard Lewis bases and stabilize the higher oxidation states.

In light of the related and sometimes contrasting features of the dithiolene and catecholate ligands, we set out to further explore the chemistry of the mixed O,S donor, mp^{2-}, and its methyl derivative, mmp^{2-} ($mmpH_2$ = 2-mercapto-4-methylphenol), with vanadium. In particular we were interested in (i) the ability of this ligand to displace oxygen donors (including the tightly held vanadyl(IV) oxygen) from oxovanadium(IV), (ii) the coordination geometry, electronic structure and redox behavior of the monomeric six-coordinate tris-complex of mp^{2-} with V(IV), and (iii) the synthesis and properties of the oxovanadium bis-complex. We report herein the synthesis (from an oxovanadium precursor) of $(Et_3NH)_2[V(mp)_3]$ and the synthesis and crystal structure of its analogue, $(Et_3NH)(PNP)[V(mmp)_3]$, together with evidence for the reversible chemical oxidation of $[V(mp)_3]^{2-}$ to $[V(mp)_3]^-$. These results represent the first isolation of a mononuclear, "bare" V(IV) complex with a mixed O,S donor ligand and the first use of such a ligand in the displacement of the vanadyl(IV) oxygen. We also report the synthesis and crystal structure of $Na(Ph_4P)[VO(mp)_2]\cdot Et_2O$, a novel oxovanadium (IV) complex of 2-mercaptophenol, as well as the characterization of these materials by infrared and electronic spectroscopies, magnetic susceptibility, EPR spectroscopy, and cyclic voltammetry.

Experimental Section

All operations were carried out under purified nitrogen or argon atmospheres using standard inert atmosphere techniques. 2-Mercaptophenol and 2-mercapto-4-methylphenol were prepared by a literature synthesis.[22] Reagents vanadyl acetylacetonate, $[VO(acac)_2]$, triethylamine, tetraphenylphosphonium chloride, and bis(triphenylphosphine)-iminium chloride (PNPCl) were purchased from Aldrich Chemical Co. and used as received. Solvents were distilled under nitrogen using conventional drying agents (EtOH over $Mg(OEt)_2$, MeOH over $Mg(OMe)_2$, MeCN over CaH_2, Et_2O over sodium/benzophenone). Triethylamine was distilled from BaO.

Elemental analyses (C, H, and N) were performed by Oneida Research Services, Whitesboro, NY. Metal analysis was performed in house using ICP-AES on DMF solutions or ICP-MS on acidic aqueous digests.

Preparation of Complexes. (a) $(Et_3NH)_2[V(mp)_3]$ (1). 2-Mercaptophenol (3.40 g, 26.9 mmol) was reacted with $VO(acac)_2$ (2.01 g, 7.57 mmol) in MeCN (80 mL) for 30 min to give a dark, red-purple solution. Et_3N (7.52 mL, 54.0 mmol) was slowly added, resulting in a color change to dark blue-green. The mixture was stirred overnight, and the solvent subsequently removed in vacuo to leave a dark blue-green oil. The oil was stirred with 10 mL of MeOH to produce a blue-black crystalline solid product, which was filtered, washed with Et_2O, and dried in vacuo; yield 4.1 g (86%). Portions of the product were recrystallized from acetone/Et_2O or MeCN/Et_2O to yield analytically pure blue-black microcrystalline solid, which was used for subsequent measurements. The IR spectrum showed no evidence of V=O at ca. 940 cm^{-1}. Anal. Calcd for $C_{30}H_{44}N_2O_3S_3V$: C, 57.39; H, 7.06; N, 4.46; S, 15.32; V, 8.11. Found: C, 57.31; H, 7.12; N, 4.50; S, 14.80; V, 8.19. Single crystals could be grown from a variety of solvent systems, but none were of sufficient quality for X-ray structure determination.

(b) $(Et_3NH)(PNP)[V(mmp)_3]$ (2). $(Et_3NH)_2[V(mmp)_3]$ was prepared by a similar procedure to that of **1** but using 2-mercapto-4-methylphenol in place of 2-mercaptophenol. One of the Et_3NH^+ cations was exchanged for the PNP^+ cation by the following procedure: After removal of solvent from the reaction mixture and addition of 10 mL of MeOH, a dark blue-green solution resulted. This was filtered, and an additional 30 mL of MeOH added, followed by an amount of PNPCl (approximately 1 mol equiv per mol of vanadium). The product was precipitated by addition of Et_2O as a crystalline, dark blue-black solid, **2**, mixed with $(Et_3NH)_2[V(mmp)_3]$. The mixture was recrystallized from MeOH/Et_2O to give pure **2** in 20% yield (based on vanadium). The IR spectrum showed no evidence of V=O at ca. 940 cm^{-1}. Anal. Calcd for $C_{63}H_{64}N_2P_2O_3S_3V$: C, 68.39; H, 5.84; N, 2.53. Found: C, 68.25; H, 5.58; N, 2.12. Slow diffusion of Et_2O into a MeOH solution of **2** afforded black crystals suitable for X-ray diffraction measurements.

(c) $Na(Ph_4P)[VO(mp)_2]\cdot Et_2O$ (3). To a stirred suspension of $VO(acac)_2$ (0.60 g, 2.3 mmol) in 30 mL of EtOH was added a solution of Na_2mp in EtOH (prepared from reaction of 0.71 g (5.6 mmol) of 2-mercaptophenol with NaOEt in EtOH). The $VO(acac)_2$ dissolved in the reaction mixture, and an olive-green solution resulted. After 4 h of stirring at ambient temperature, the mixture was filtered to remove small amounts of undissolved material, and 1.5 g of Ph_4PCl was added (4.0 mmol) to precipitate the product as a pale green solid, contaminated with NaCl. The solid was filtered and subsequently taken up in 45 mL of MeCN and filtered to remove a small amount of pale solid (NaCl). Addition of Et_2O to the green filtrate led, after overnight standing, to precipitation of dark green crystalline solid **3**; yield 1.12 g (72%). The IR spectrum showed a strong band at 940 cm^{-1} indicative of the presence of the V=O group. Anal. Calcd for $C_{40}H_{38}PO_4S_2NaV$: C, 63.91; H, 5.09; N, 0; V, 6.78. Found: C, 63.91; H, 4.98; N, 0.25; V, 6.39. One preparation afforded some well-formed diamond-

(12) (a) Higes-Rolando, F. J.; Perez-Florindo, A.; Valenzuela-Calahorro, C.; Martin-Ramos, J. D.; Romero-Garzon, J. *Acta Crystallogr.* **1994**, *C50*, 1049−1052. (b) Tsagkalidis, W.; Rodewald, D.; Rehder, D.; Vergopoulos, V. *Inorg. Chim. Acta* **1994**, *219*, 213−215.
(13) Kang, B.; Weng, L.; Liu, H.; Wu, D.; Huang, L.; Lu, C.; Cai, J.; Chen, X.; Lu, J. *Inorg. Chem.* **1990**, *29*, 4873−4877.
(14) Weng, L. H.; Kang, B. S.; Chen, X. T.; Hong, M. C.; Lei, X. J.; Hu, Y. H.; Liu, H. Q. *Chin. J. Chem.* **1993**, *11*, 30−39.
(15) Eisenberg, R. *Prog. Inorg. Chem.* **1970**, *12*, 295 and references therein.
(16) Pierpont, C. G.; Lange, C. W. *Prog. Inorg. Chem.* **1994**, *41*, 331−442.
(17) Pierpont, C. G.; Buchanan, R. M. *Coord. Chem. Rev.* **1981**, *38*, 45−87.
(18) (a) Nardillo, A. M.; Catoggio, J. A. *Anal. Chim. Acta* **1975**, *74*, 85. (b) Lobinski, R.; Marczenko, Z. *Anal. Chim. Acta* **1989**, *226*, 281.
(19) Michibata, H.; Sakurai, H. in *Vanadium in Biological Systems*; Chasteen, N. D., Ed.; Kluwer: Dordrecht, 1990; p 153.
(20) Luneva, N. P.; Nikonova, L. A.; Shilov, A. E. *Kinet. Katal.* **1980**, *21*, 1041.
(21) Galeffi, B.; Postel, M.; Grand, A.; Rey, P. *Inorg. Chim. Acta* **1989**, *160*, 87.
(22) Cabiddu, S.; Maccioni, A.; Secci, M. *Gazz. Chim. Ital.* **1969**, *99*, 1095−1106.

shaped green crystals from the final MeCN/Et_2O recrystallization, and these were used for X-ray data collection.

Physical Measurements. Infrared spectra were obtained as KBr pellets on a Nicolet 5PC FTIR spectrometer. Electronic spectra were obtained on MeCN or MeOH solutions in gas-tight quartz cuvettes using a Perkin-Elmer Lambda 3B UV−vis spectrophotometer. Magnetic susceptibility measurements were conducted on powdered samples at ambient temperature using a Johnson Matthey Mark II magnetic susceptibility balance. EPR spectra were recorded on MeCN solutions at ambient temperature using a Varian E112 spectrometer with DPPH as calibrant ($g = 2.0037$) and on frozen MeCN solutions at ca. 77 K using a Varian Century-Line spectrometer. The EPR spectra were fit by a computer program that included *g*-strain statistical considerations, but the Hamiltonian contained only the magnetic hyperfine interaction in addition to the electron Zeeman: $H = \hat{g}\beta Hm_s + \hat{a}m_s m_I$, where $\hat{g}$ is the effective *g*-value at the particular orientation of the applied magnetic field in *g*-frame and $\hat{a}$ is the effective *a*-value at the same orientation. This approximation ignores the nuclear quadrupole interaction and the higher-order terms in the magnetic hyperfine interaction. These corrections are expected to be small because they are approximately equal to $(a/2g\beta H)^2$ or 2×10^{-4} in the case of these vanadium complexes. The ability of this program to simulate the EPR spectra of these compounds is shown in Figure 6 with the fitting parameters given in Tables 7 and 8. Electrochemical measurements were performed on MeCN solutions (ca. 4 mM) using a BAS 100B electrochemical analyzer; a platinum disk working electrode was used in conjunction with a platinum wire auxiliary electrode and a Ag/AgCl reference electrode. The solutions contained 0.1 M tetra-*n*-butylammonium perchlorate as supporting electrolyte.

X-ray Diffraction and Structure Solution. Intensity data were collected at low temperature using a Syntex $P2_1$ diffractometer under the control of a Siemens P3/PC microcomputer system. Data collection parameters are detailed in Table 1. Both crystal structures were solved using a combination of direct methods and difference-Fourier interpretation utilizing the SHELXTL Plus program set.[23] Both structures were refined using the F^2 values of all data employing the program SHELXL-93.[24] Each data set was corrected for absorption *via* semiempirical psi-scans and for the effects of primary and secondary extinction. Refinement statistics are shown in Table 1.

(a) $(Et_3NH)(PNP)[V(mmp)_3]$ (2) crystallized in the polar orthorhombic space group $Pna2_1$. Direct methods yielded the initial locations of all non-hydrogen atoms. Full-matrix least-squares, with polar axis restraints applied by the method of Flack and Schwarzenbach,[25] converged uneventfully, after which hydrogen atoms were placed in idealized positions. The hydrogen atom positions were allowed to ride on the corresponding carbon atoms with the U_{eq} values set equal to 1.2 or 1.5 times the equivalent isotropic *U* values of the associated carbons. The hydrogen atom of the triethylammonium ion, H(2), was located from the difference-Fourier map after a high angle refinement. After all non-hydrogen atoms were refined anisotropically to convergence, the position of the triethylammonium hydrogen was allowed to refine. The isotropic *U* value of H(2) was set to 1.2 times the U_{eq} of N(2).

(b) $Na(Ph_4P)[VO(mp)_2]\cdot Et_2O$ (3) crystallized in the triclinic space group $P\bar{1}$. Direct methods revealed the anion structure, the sodium ion, and the tetraphenylphosphonium ion. After initial full-matrix least-squares refinement, the cation exhibited a distorted phenyl group suggestive of rotational disorder. Application of similar distance and planarity restraints stabilized the further refinement of the static rotamer. The ortho and meta carbons of one component were refined with a common, variable site occupancy factor, yielding a value of 56.265%, with the site occupancy factor of the other component set to one minus the free variable.

Hydrogen atoms, including those of the disordered group, were placed in ideal positions and refined *via* a riding model with the isotropic *U* values set to 1.2 times the U_{eq} values of the respective carbons. All non-hydrogen atoms were refined anisotropically except the carbons of the disordered group.

Further analysis, however, showed significant electron density about the sodium ion. Five peaks were chosen, with those of a reasonable distance from sodium, 2.2−2.4 Å, labeled as oxygen. The remaining three peaks were named as carbon atoms. The ether atoms were refined isotropically without the addition of hydrogen atoms or the application of similar distance restraints. The group was refined with a common, variable site occupancy factor giving a value of 72.046%. Since the geometry of the anion was not influenced by the disordered solvent, a more elaborate disorder model was judged unnecessary.

Table 1. Crystallographic Data for **2** and **3**

	2 = $(Et_3NH)(PNP)[V(mmp)_3]$	**3** = $Na(Ph_4P)[VO(mp)_2]\cdot Et_2O$
formula	$C_{63}H_{64}N_2O_3P_2S_3V$	$C_{38.12}H_{28}NaO_{4.41}PS_2V$
crystal system	orthorhombic	triclinic
space group	$Pna2_1$	$P\bar{1}$
a, Å	23.974(7)[a]	12.185(4)[b]
b, Å	9.569(4)	12.658(4)
c, Å	25.101(6)	14.244(4)
α, deg		103.19(2)
β, deg		100.84(2)
γ, deg		114.17(2)
V, Å^3	5758(2)	1851.2(9)
Z	4	2
D_{calc}, g/cm^3	1.276	1.302
crystal size, mm	1.80 × 0.54 × 0.46	0.58 × 0.58 × 0.24
wavelength (Mo Kα), Å	0.71073	0.71073
F(000)	2324	746
abs coeff, mm^{-1}	0.383	0.474
min and max transmn	0.797, 0.726	0.856, 0.771
temp, K	110	138
scan type	*ω*	*ω*
scan range, deg	2.00	2.00
scan speed, deg/min	8.37	8.37
2*θ* range	3.5 to 50.0	3.5 to 45.0
range of *h*, *k*, *l*	−8 to 28, −11 to 10, −29 to 8	−1 to 13, −13 to 12, −15 to 15
no. of reflns collected	6224	5658
no. of unique reflns	5091	4836
no. of obsd reflns ($F_o > 4\sigma(F_o)$)	4575	3874
data/restraints/params	5312/1/671	4836/97/416
R1 ($F_o > 4\sigma(F_o)$),[c] %	3.24	8.10
*w*R2 (all data),[d] %	7.36	25.51
goodness of fit (on F^2)[e]	1.008	1.041
weighting scheme	$w = 1/[\sigma^2(F_o^2) + (0.0417P)^2 + 0.0000P)$	$w = 1/[s^2(F_o^2) + (0.1637P)^2 + 7.3622P]$
extinction coefficient[f]	0.0003(3)	0.004(2)

[a] 22 reflections, $20 \le 2\theta \le 30°$. [b] 33 reflections $5.0 \le 2\theta \le 30°$. [c] $R1 = \sum||F_o| - |F_c||/|F_o|$. Conventional *R*-factors are calculated using the observed criterion. This criterion is irrelevant to the choice of reflections used in the refinement. [d] $wR2 = [\sum[w(F_o^2 - F_c^2)^2]/\sum[w(F_o^2)^2]]^{1/2}$. Weighted *R*-factors are based on F^2 and are statistically about twice as large as those based on *F*. [e] $S = [\sum[w(F_o^2 - F_c^2)^2]/(n - p)]^{1/2}$. The goodness of fit is based on F^2 where n = number of data and p = number of parameters refined. [f] An extinction parameter, *x*, is refined where F_c is multiplied by $k[1 + 0.001xF_c^2\lambda^3/\sin(2\theta)]^{-1/4}$ with k = overall scale factor.

Results and Discussion

Syntheses. In the preparation of **1** and **2** from $VO(acac)_2$, the mp and mmp ligands are able, under mild, anaerobic conditions, to displace the oxo group as well as the acac group, resulting in the tris-complexes. Displacement of the vanadyl oxygen has been demonstrated previously in the syntheses of tris(catecholate)vanadium(IV) complexes[26a] and also in the

(23) Copyright 1989, 1990, Siemens Analytical X-Ray Instruments Inc., Madison, WI 53719.
(24) Sheldrick, G. M. *SHELXL-93, Program for the refinement of crystal structures*; University of Gottingen, Germany, 1993.
(25) Flack, H. D.; Schwarzenbach, D. *Acta Crystallogr.* **1988**, *A44*, 499−506.
(26) (a) Cooper, S. R.; Koh, Y. B.; Raymond, K. N. *J. Am. Chem. Soc.* **1982**, *104*, 5092−5102. (b) Branca, M.; Micera, G.; Dessi, A.; Sanna, D.; Raymond, K. N. *Inorg. Chem.* **1990**, *29*, 1586−1589.

preparation of $V^{IV}(sal\text{-}NSO)_2$,[27] in which a sulfur donor is incorporated in a tridentate ligand. These reactions are facilitated by the use of the ligand in its protonated form and the addition of a mild base (Et_3N) in the case of **1**, **2**, and the tris(catecholates), or no base at all in the case of $V^{IV}(sal\text{-}NSO)_2$. Under these conditions the oxo group may be protonated and released as water or hydroxide (eq 1).

$$VO(acac)_2 + 3mpH_2 + 2Et_3N \longrightarrow [V(mp)_3]^{2-} + 2acacH + H_2O + 2Et_3NH^+ \quad (1)$$

1

By contrast, in previous syntheses of non-oxo vanadium complexes with sulfur donors (and with the metal in the formal oxidation state (IV)), such as trinuclear $[V_3(mp)_6]^-$,[13] dimeric $[V(mp)_3NaLL']_2^{2-}$,[14] dithiolene complexes $[V(DDDT)_3]^{2-}$ [28] (DDDT = 5,6-dihydro-1,4-dithiin-2,3-dithiolato), $[V(dmt)_3]^{2-}$ [29] (dmt = 1,2-dithiole-3-thione-4,5-dithiolato), and $[V(mnt)_3]^{2-}$ [30a] (mnt = 1,2-dicyanoethylene-1,2-dithiolato), and thiolate complex $V(SBu^t)_4$,[31] the source of vanadium employed was invariably VCl_3 and oxidation to V(IV) occurred. The use of oxovanadium(IV) starting materials in the syntheses of non-oxo vanadium(IV) products depends not only on appropriate choice of reaction conditions but also on the ability of the chosen ligand to donate sufficient electron density (σ and π) to the metal to stabilize the non-oxo product. Destabilization of a V=O unit has also been shown to occur upon reduction to V(III) as in the conversion of $[VO(edt)_2]^{2-}$ to $[V_2(edt)_4]^{2-}$ by acenaphthylenide anion in the presence of protons.[32] While the conventional view of vanadium in higher oxidation states is of a hard Lewis acid, preferring to bind to O and N donors,[33] it has become clear that sulfur-containing ligands are eminently capable, under the right conditions, of displacing oxygen donors from vanadium(IV), including the normally tightly held vanadyl oxygen.

Efforts to obtain diffraction quality crystals of compounds containing $[V(mp)_3]^{2-}$ were unsuccessful despite numerous attempts with a variety of cations and solvent systems. For this reason the methylated ligand, mmp, was employed, and this, in combination with the mixed cation system Et_3NH^+/PNP^+, gave suitable crystals from which the structure of **2** could be obtained.

The conditions employed for the synthesis of **3** (use of the ligand in its deprotonated form) were such as to favor the formation of the oxovanadium(IV) product, as shown in eq 2.

$$VO(acac)_2 + 2Na_2mp \longrightarrow [VO(mp)_2]^{2-} + 2acac^- + 4Na^+ \quad (2)$$

3

Subsequent addition of a precipitating cation (Ph_4P^+), followed by recrystallization, led to the formation of crystalline **3**, in which the complex anion is found together with one Na^+, one Ph_4P^+, and one solvent molecule.

(27) Dutton, J. C.; Fallon, G. D.; Murray, K. S. *Inorg. Chem.* **1988,** *27*, 34.
(28) Welch, J. H.; Bereman, R. D.; Singh, P. *Inorg. Chem.* **1988**, *27*, 2862−2868.
(29) Olk, R.-M.; Dietzsch, W.; Kirmse, R.; Stach, J.; Hoyer, E. *Inorg. Chim. Acta* **1987**, *128*, 251−259.
(30) (a) Stiefel, E. I.; Dori, Z.; Gray, H. B. *J. Am. Chem. Soc.* **1967**, *89*, 3353. (b) Kwik, W.-L; Stiefel, E. I. *Inorg. Chem.* **1973**, *12*, 2337. (c) Atherton, N. M.; Winscom, C. J. *Inorg. Chem.* **1973**, *12*, 383−390.
(31) Heinrich, D. D.; Folting, K.; Huffman, J. C.; Reynolds, J. G.; Christou, G. *Inorg. Chem.* **1991**, *30*, 300−305.
(32) Christou, G.; Heinrich, D.; Money, J. K.; Rambo, J. R.; Huffman, J. C.; Folting, K. *Polyhedron* **1989**, 1723.
(33) Greenwood, N. N.; Earnshaw, A. *Chemistry of the Elements*; Pergamon Press: New York, 1984; p 1159.

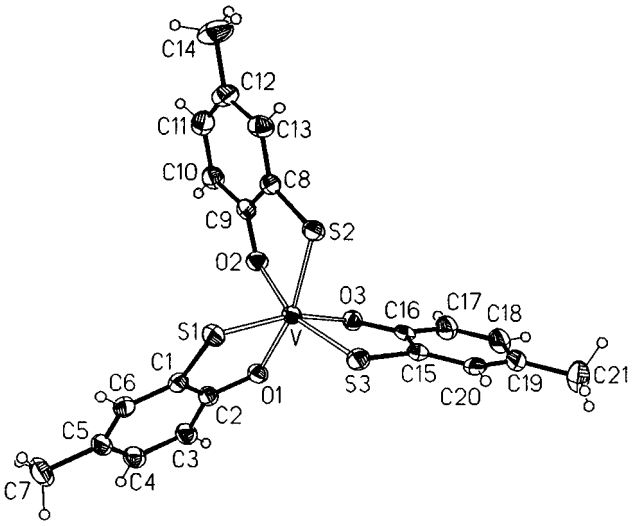

Figure 1. Structure and numbering scheme of the anion in **2**. Thermal ellipsoids are drawn at 50% probability.

Table 2. Selected Fractional Coordinates ($\times 10^4$) of Non-Hydrogen Atoms in **2**

	x	*y*	*z*	*U*eq
		$V(mmp)_3$		
V	3323(1)	4769(1)	3268(1)	22(1)
S(1)	3006(1)	6352(1)	3925(1)	27(1)
S(2)	3277(1)	6593(1)	2630(1)	27(1)
S(3)	4244(1)	5581(1)	3368(1)	29(1)
O(1)	3184(1)	3417(3)	3832(1)	25(1)
O(2)	2615(1)	4313(3)	2948(1)	28(1)
O(3)	3692(1)	3258(3)	2886(1)	25(1)
C(1)	2788(2)	5116(4)	4399(2)	25(1)
C(2)	2922(2)	3731(4)	4290(1)	26(1)
C(3)	2806(2)	2723(5)	4671(2)	30(1)
C(4)	2539(2)	3090(5)	5146(2)	32(1)
C(5)	2389(2)	4430(5)	5248(2)	32(1)
C(6)	2521(2)	5454(5)	4870(2)	30(1)
C(7)	2105(2)	4839(6)	5767(2)	49(1)
C(8)	2587(2)	6335(4)	2422(1)	26(1)
C(9)	2329(2)	5163(4)	2631(1)	25(1)
C(10)	1769(2)	4905(5)	2496(2)	33(1)
C(11)	1488(2)	5834(6)	2163(2)	40(1)
C(12)	1746(2)	6998(5)	1949(2)	36(1)
C(13)	2307(2)	7243(5)	2079(2)	33(1)
C(14)	1451(2)	8000(6)	1578(2)	57(2)
C(15)	4566(2)	4397(4)	2929(2)	25(1)
C(16)	4233(2)	3324(4)	2735(1)	26(1)
C(17)	4466(2)	2340(5)	2391(2)	38(1)
C(18)	5020(2)	2434(6)	2249(2)	44(1)
C(19)	5358(2)	3492(6)	2442(2)	42(1)
C(20)	5127(2)	4475(5)	2781(2)	34(1)
C(21)	5969(2)	3569(6)	2285(2)	59(2)
		Et_3NH		
N(2)	2971(2)	10940(4)	3156(1)	33(1)
C(58)	3010(2)	10468(5)	2587(2)	43(1)
C(59)	2695(2)	11425(5)	2207(2)	48(1)
C(60)	2384(2)	11133(5)	3347(2)	50(1)
C(61)	2039(2)	9825(6)	3324(3)	68(2)
C(62)	3293(2)	9974(5)	3513(2)	46(1)
C(63)	3908(2)	10009(6)	3426(2)	58(2)

Description of Structures. $(Et_3NH)(PNP)[V(mmp)_3]$ (2). The X-ray structure of the tris complex $(Et_3NH)(PNP)[V(mmp)_3]$ (**2**) shows the anion $[V(mmp)_3]^{2-}$ associated with the Et_3NH^+ cation through hydrogen bonding. The other cation, PNP^+, is a discrete unit. The cations have normal structures and will not be discussed further. The molecular structure and numbering scheme for the anion $[V(mmp)_3]^{2-}$ of **2** are shown in Figure 1. Fractional atomic coordinates are in Table 2 and selected structural parameters in Table 4.

The vanadium is coordinated by three bidentate chelating mmp^{2-} ligands binding through three oxygen and three sulfur atoms. The coordination geometry around the vanadium(IV) is between octahedral and trigonal prismatic, with the two triangular faces of the distorted polyhedron being comprised of three sulfur atoms and three oxygen atoms, respectively, in a pseudofacial arrangement. The symmetry of the anion closely approaches C_3, with the 3-fold axis perpendicular to the S_3 and O_3 planes. Two commonly used measures of distortion between idealized octahedral (O_h, or D_{3d} with trigonal distortion) and idealized trigonal prismatic (D_{3h}) geometries are the trans angle and the twist angle. In Table 5 comparison is made between **2** and related compounds for these angles and other pertinent structural parameters.

The average S−V−O trans angle in **2** of 164.1° is between the values of 180° for a perfect octahedron (172° if correction is made[34,35] for an average bite angle S−V−O of 82.0°) and 136° for a perfect trigonal prism. It is close to the value of 162.8° reported[26a] for the trans angle in $[V(cat)_3]^{2-}$, described as distorted octahedral. The two dianionic vanadium tris(dithiolenes) $[V(dmt)_3]^{2-}$ [29] and $[V(mnt)_3]^{2-}$ [30a] have trans angles of 164.3° and 158.6°, respectively, and both are described as distorted octahedral. In **2** the triangular planes O_3 and S_3 are not perfectly parallel, but tilted at an angle of 4.4(1)°. The average projected twist angle between these two planes is 40.8°, which is between the ideal values of 0° for trigonal prismatic and 60° for octahedral geometries and can be compared to ∼39° in distorted octahedral $[V(cat)_3]^{2-}$ [26a] and 3.7° in slightly distorted trigonal prismatic $[V(DDDT)_3]^{-}$.[28]

The dihedral angles between O−V−S planes and the aromatic rings are 7.0(1)°, 12.5(2)°, and 10.7(2)° for rings 1 through 3, respectively, averaging to 10.0(2)°. This bending of the ligand planes can be compared with the averaged values of 7.7° in $[V(cat)_3]^{2-}$,[26a] 21.4° in $Mo(S_2C_6H_4)_3$,[35] and 22.4° in $[Nb(S_2C_6H_4)_3]^{-}$,[36] where the ligands are analogous to mmp^{2-}. The angle diminishes as the complexes approach the octahedral limit, and this has been discussed[28] in terms of π overlap of the metal and ligand orbitals. The dihedral angles between ligand planes 1 and 2, 2 and 3, and 1 and 3 are 81.63(6)°, 76.29(6)°, and 60.3(7)°, respectively. The averaged bite angle of 82.0° is similar to that of other six coordinate complexes[14,37] of mp^{2-}.

The hydrogen bonding of the Et_3NH^+ cation to the O atoms of ligands 1 and 3 is shown in Figure 2. Ligand 2 has a N(2)···O(2) distance of 3.379(5) Å, outside of the normal H-bonding range[38] of 2.81−3.04 Å for N−H···O. Some slight differences in structural parameters between ligand 2 and ligands 1 and 3 such as bond lengths V−O and C−O (Table 4) are too small to represent a quinone or semiquinone contribution to the bonding and may be attributable to the close approach of the Et_3NH^+ cation to ligands 1 and 3.

The structure of the anion in **2** is very similar to that of the $[V(mp)_3]^{2-}$ unit in dimeric $(Et_4N)_2[V(mp)_3Na(MeOH)_2]_2$.[14] Such small differences as those that occur between these two structures can be most reasonably attributed to the different influences of the hydrogen-bonded Et_3NH^+ in **2** *vs* the coordinated Na^+ in $(Et_4N)_2[V(mp)_3Na(MeOH)_2]_2$. For example, the average O−V−O bond angle and S−V−O cis angle in **2** are 89.4° and 103.4°, respectively, compared to 88.3° and 106.6° in $(Et_4N)_2[V(mp)_3Na(MeOH)_2]_2$, reflecting a slight displacement

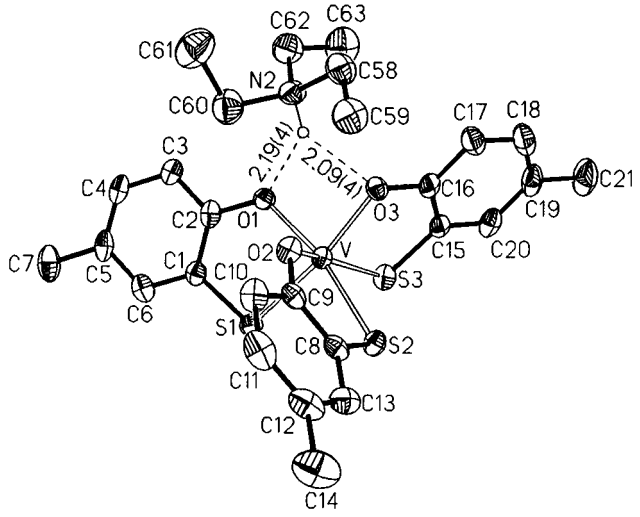

Figure 2. Hydrogen bonding of the Et_3NH cation to the anion of **2**. Thermal ellipsoids are drawn at 50% probability. All hydrogen atoms except H(2) of the cation are omitted for clarity. Additional distances (Å) are N(2)−O(1) = 2.960(4) and N(2)−O(3) = 2.892(5). Angles (deg) are given as H(2)−O(1)−V = 87(1), H(2)−O(3)−V = 90(1), N(2)−H(2)−O(1) = 138(4), N(2)−H(2)−O(3) = 142(4), and O(1)−H(2)−O(3) = 77(2).

of the ligand O atoms toward the bridging Na^+ ions. A much greater difference occurs between **2** and $(Et_4N)[V_3(mp)_6]$[13] (average O−V−O and cis S−V−O angles of 77.5° and 111.2°, respectively), a result of the stronger coordination of the ligand oxygens to the V(III) which bridges the two $[V(mp)_3]^{2-}$ units in the trinuclear complex. The presence of the methyl group on the ligand mmp^{2-} in **2** does not appear to be of any structural significance since such bond lengths as might be expected to be affected (e.g. C−O and C−S) are virtually identical between **2** and $(Et_4N)_2[V(mp)_3Na(MeOH)_2]_2$.

(b) $Na(Ph_4P)[VO(mp)_2]\cdot Et_2O$ (3). The X-ray crystal structure of **3** shows two $[VO(mp)_2]^{2-}$ anions per unit cell related through a crystallographic inversion center and linked through a pair of Na^+ ions. The sodium ions are related through the inversion center, and each sodium ion is coordinated by three ligand oxygen atoms (O(1), O(2), O(1#1)), one vanadyl oxygen atom (O(3#1)), and one oxygen atom from diethyl ether. The diethyl ether molecule displays considerable static disorder, and rotational disorder was evident in one of the phenyl rings in the Ph_4P^+ cation (two per unit cell). These disorders were modeled by the methods described in the Experimental Section. Other than this disorder, the Ph_4P^+ cations were unremarkable. Neither of the two disorder problems had any bearing on the structure of the $[VO(mp)_2]^{2-}$ ion of interest. The molecular structure and numbering scheme for the dimeric unit consisting of the pair of vanadyl(IV) anions, $[VO(mp)_2]^{2-}$, and sodium ions are shown in Figure 3. Fractional atomic coordinates are in Table 3 and selected structural parameters in Table 4.

The anion has the expected square pyramidal coordination geometry, with the two chelate rings in the cis configuration (Figure 4). The same cis configuration is found in the other two structurally characterized oxovanadium(IV) complexes with a O_2S_2 donor set in the basal plane.[12,39] The idealized symmetry of the VO_2S_2 core is C_s, with the mirror plane passing through the apical V−O(3) bond and bisecting the O(1)···O(2) and S(1)···S(2) vectors. The vanadium atom is displaced toward the apical oxygen by 0.638(2) Å from the O_2S_2 least-squares

(34) Brown, G. F.; Stiefel, E. I. *Inorg. Chem.* **1973**, *12*, 2140.
(35) Cowie, M.; Bennett, M. J. *Inorg. Chem.* **1976**, *15*, 1595.
(36) Cowie, M.; Bennet, M. J. *Inorg. Chem.* **1976**, *15*, 1589 and references therein.
(37) Hu, Y. H.; Weng, L. H.; Kang, B. S. *Jiegou Huaxue* **1991**, *10*, 84.
(38) Wells, A. F. *Structural Inorganic Chemistry*, 4th ed.; Oxford University Press: Oxford, 1975.
(39) Preuss, F.; Steidel, M.; Exner, R. *Z. Naturforsch, B* **1990**, *45*, 1618−1624.

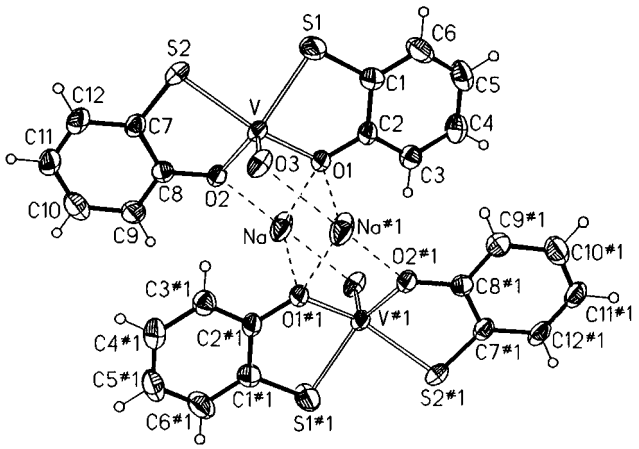

Figure 3. Structure of the centrosymmetric anion and sodium ion complex of **3**. Thermal ellipsoids are drawn at 50% probability. The disordered ether molecules are omitted for clarity. The symmetry transformation used to generate equivalent atoms is given as #1 = 1 − *x*, 2 − *y*, −*z*.

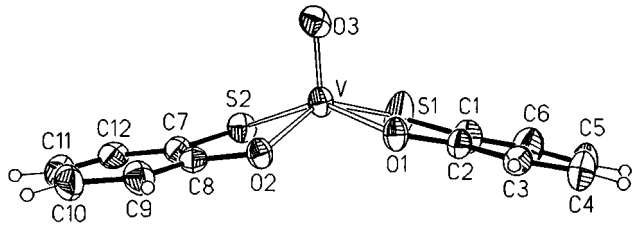

Figure 4. Depiction of the ligand bending of the $[VO(mp)_2]^{2-}$ ion of **3**. Thermal ellipsoids are drawn at 50% probability. The sodium ion and coordinated ether molecule are omitted for clarity.

Table 3. Selected Fractional Coordinates ($\times 10^4$) of Non-Hydrogen Atoms in **3** for $[NaVO(mp)_2]^-$

	x	*y*	*z*	U_{eq}
V	3887(1)	9458((1)	1455(1)	28(1)
S(1)	1646(2)	8331(2)	917(2)	61(1)
S(2)	3935(2)	9049(2)	2996(1)	35(1)
O(1)	3644(4)	8852(4)	−11(3)	31(1)
O(2)	5401(4)	9253(4)	1611(3)	30(1)
O(3)	4302(5)	10899(4)	1691(3)	39(1)
C(1)	1405(7)	7904(7)	−404(5)	38(2)
C(2)	2483(6)	8236(6)	−714(5)	30(2)
C(3)	2347(7)	7941(6)	−1746(5)	34(2)
C(4)	1157(8)	7299(7)	−2459(6)	48(2)
C(5)	88(8)	6948(8)	−2159(6)	54(2)
C(6)	224(7)	7252(8)	−1130(6)	51(2)
C(7)	5530(6)	9333(6)	3317(5)	31(2)
C(8)	6084(6)	9415(6)	2546(5)	30(2)
C(9)	7349(7)	9664(6)	2756(6)	39(2)
C(10)	8023(7)	9844(7)	3752(7)	50(2)
C(11)	7464(8)	9756(6)	4485(6)	43(2)
C(12)	6224(7)	9501(6)	4280(5)	38(2)
Na	5583(3)	8898(4)	−20(2)	58(1)

plane, and the largest deviation from this plane is 0.057(2) Å for O(2). Structural features of **3** are compared with related compounds in Table 5. The vanadyl V═O bond length of 1.611(5) Å is within the reported range of oxovanadium complexes possessing catecholate,[26a] dithiolate,[40] N_2S_2,[27] or O_2S_2[12,39] donor sets (1.593−1.642 Å; Table 5). The basal plane V−O bonds average to 1.959 Å, which is only slightly longer than the average V−O bond length in **2** (1.940 Å) and very close to the basal plane V−O bond distances in related

(40) (a) Money, J. K.; Huffman, J. C.; Christou, G. *Inorg. Chem.* **1985**, *24*, 3297−3302. (b) Money, J. K.; Folting, K.; Huffman, J. C.; Collison, D.; Temperley, J.; Mabbs, F. E.; Christou, G. *Inorg. Chem.* **1986**, *25*, 4583.

Table 4. Selected Bond Lengths (Å) and Angles (deg) in $[V(mmp)_3]^{2-}$ of **2** and $[VO(mp)_2]^{2-}$ of **3**

$[V(mmp)_3]^{2-}$

Bond Lengths

V−O(1)	1.947(3)	S(1)−C(1)	1.756(4)
V−O(2)	1.927(3)	S(2)−C(8)	1.753(4)
V−O(3)	1.947(3)	S(3)−C(15)	1.759(4)
V−S(1)	2.365(1)	O(1)−C(2)	1.346(4)
V−S(2)	2.370(1)	O(2)−C(9)	1.330(4)
V−S(3)	2.354(1)	O(3)−C(16)	1.353(4)

Bond Angles

O(1)−V−O(3)	86.7(1)	O(2)−V−O(1)	90.2(1)
O(2)−V−O(3)	91.5(1)		

Trans Angles

O(1)−V−S(2)	166.59(8)	O(3)−V−S(1)	164.77(8)
O(2)−V−S(3)	160.93(9)		

Twist Angles[a,b]

O(1)−centO$_3$−centS$_3$−S(1)	42.0
O(2)− centO$_3$−centS$_3$−S(2)	43.3
O(3)−centO$_3$−centS$_3$−S(3)	37.1

Cis Angles

O(1)−V−S(3)	107.51(8)	O(3)−V−S(2)	103.61(9)
O(2)−V−S(1)	98.77(9)		

Bite Angles

O(1)−V−S(1)	82.15(9)	O(3)−V−S(3)	82.63(8)
O(2)−V−S(2)	81.11(9)		

$[VO(mp)_2]^{2-}$

Bond Lengths

Na−O(1)	2.342(5)	Na−O(3)#1	2.475(5)
Na−O(2)	2.334(5)	Na···Na#1	3.606(7)
Na−O(1)#1	2.594(6)		

Vanadyl Bond

V−O(3)	1.611(5)

Basal Plane

V−O(2)	1.946(4)	V−S(2)	2.364(2)
V−O(1)	1.972(4)	V−S(1)	2.367(3)

Bond Angles

V−O(1)−C(2)	122.0(4)	V−S(1)−C(1)	97.1(2)
V−O(2)−C(8)	119.3(4)	V−S(2)−C(7)	95.5(2)

Bite Angles

O(1)−V−S(1)	83.4(1)	O(2)−V−S(2)	83.5(1)

[a] Dymock, K. R.; Palenik, G. J. *Inorg. Chem.* **1975**, *14*, 1220−1222. [b] centS$_3$ and centO$_3$ are unweighted centroids of the triangular planes S$_3$ and O$_3$. The *x*, *y*, *z* coordinates ($\times 10^4$) are given as 0.35088, 0.61752, 0.33078 and 0.31636, 0.36623, 0.32220, respectively.

oxovanadium(IV) complexes (Table 5). The basal plane V−S bonds average to 2.365 Å, almost identical to the average V−S bond length in **2** (2.363 Å) and again close to V−S distances in related oxovanadium(IV) complexes (Table 5). In complexes **2** and **3**, the average of the V−O−C angles (123.5° in **2**; 120.6° in **3**) suggests that sp^2 hybrid orbitals are used by ligand O atoms, while the average of the V−S−C angles (97.9° in **2**; 96.3° in **3**) suggests predominantly p orbitals are used by S. In **3** the two O−V−S planes make an angle of 47.1(2)°, while the V−O−C−C−S chelate rings are folded about the O−S vector, with the aromatic rings bending toward the apical O and making angles of 6.3(2)° and 21.9(2)° with the O(1)−V−S(1) and O(2)−V−S(2) planes, respectively (Figure 4). The bending about the O(2)−S(2) vector is substantially larger than the bending about the O(1)−S(1) vector, and this prevents extension of the C_s symmetry of the core to the entire anion.

IR and UV−Vis Spectroscopies. The most pertinent difference between the infrared spectra of the tris-complexes **1** and **2** and the vanadyl bis-complex **3** is the presence of the V═O stretch at 940 cm^{-1} in the latter. This frequency is at the low

Table 5. Comparison of Distances (Å) and Angles (deg) of **2**, **3**, and Related Compounds[a]

complex	donor set	V−S	V−O	(O)S−V−O(S) (trans)	twist angle	ref
2 $[V(mmp)_3]^{2-}$	$V(OS)_3$	2.363(1)	1.940(3)	164.10(9)	40.8	this work
$[V(mp)_3Na(MeCN)(MeOH)]_2^{2-}$	$V(OS)_3$	2.369(1)	1.956(3)	159.7(1)	twisted[b]	14
$[V(cat)_3]^{2-}$	$V(OO)_3$		1.942(8)	162.8(6)	∼39	26a
$[V(mnt)_3]^{2-}$	$V(SS)_3$	2.36(1)		158.6	twisted[b]	30a
$[V(DDDT)_3]^-$	$V(SS)_3$	2.340(4)		135.5(2)	3.7	28

complex	donor set	V=O	displacement of V from basal plane	V−O (basal plane)	V−S	ref
3 $[VO(mp)_2]^{2-}$	$VO(OS)_2$	1.611(5)	0.638(2)	1.959(4)	2.365(2)	this work
$VO(C_5H_4NOS)_2$	$VO(OS)_2$	1.593(3)	0.642	1.956(3)	2.374(2)	12a
$VO[SSi(OC_4H_9)_3]_2$	$VO(OS)_2$	1.642(13)		2.106(13)	2.333(6)	39
$[VO(cat)_2]^{2-}$	$VO(OO)_2$	1.616(4)	0.58	1.956(4)		26a
$[VO(edt)_2]^{2-}$	$VO(SS)_2$	1.625(2)	0.668		2.378(1)	40a
VO(tsalen)	$VO(N_2S_2)$	1.598(6)	0.608(1)		2.346(3)	27

[a] Standard deviations of average values are those given in the original paper or the larger of the individual standard deviations. [b] No twist angle given.

Table 6. UV−Vis Spectral Features of **1**, **2**, **3**, and Related Compounds

complex	donor set	λ, nm (ϵ, L mol^{-1} cm^{-1})				solvent	ref
1 $[V(mp)_3]^{2-}$	$V(OS)_3$	738 (5300)	586 (6400)	481 (5100)	386 (7400)	MeCN	this work
2 $[V(mmp)_3]^{2-}$	$V(OS)_3$	756(4800)	594 (5900)	482 (4600)	389 (sh 6400)	MeCN	this work
$[V(cat)_3]^{2-}$	$V(OO)_3$	650 (sh 8200)	552 (9200)	∼440 (sh 6000)	∼320 (∼6000)	MeCN	26a
$[V(DDDT)_3]^{2-}$	$V(SS)_3$	660(6100)		409 (5600)	345 (sh)	DMF	28
$V(sal\text{-}NSO)_2$	$V(ONS)_2$		532 (2131)		350 (9964)	DMF	27

complex	donor set	λ, nm (ϵ, L mol^{-1} cm^{-1})			solvent	ref
3 $[VO(mp)_2]^{2-}$	$VO(OS)_2$	602 (78)	547 (92)	411 (299)	MeCN	this work
$[VO(maa)_2]^{2-}$	$VO(OS)_2$	630 (28)	570 (sh 21)		H_2O	11
$VO(PTO)_2$	$VO(OS)_2$	658 (57)	505 (76)		CH_2Cl_2	45
$[VO(cat)_2]^{2-}$	$VO(OO)_2$	656 (69)	540 (38)		H_2O	26a
$[VO(edt)_2]^{2-}$	$VO(SS)_2$	622 (75)	550 (sh 50)	400 (500)	DMF	40b
VO(tsalen)	$VO(N_2S_2)$	670 (107)	594 (181)	391 (8500)	DMF	27

end of the range 935−1035 cm^{-1} reported for a large set of oxovanadium complexes.[41] The relatively low frequency is consistent with the crystallographic results for **3**, which show a rather long V=O bond (1.611 Å as compared to 1.56−1.60 Å for most square pyramidal vanadyl(IV) complexes). The frequency of 940 cm^{-1} is substantially lower than that in $VO(C_5H_4NOS)_2$ (984 cm^{-1})[12b] and VO(tsalen) (975 cm^{-1})[27] but higher than that in $[VO(edt)_2]^{2-}$ (930 cm^{-1} for the Me_4N^+ salt and 909 cm^{-1} for the Ph_4P^+ salt)[40a] in keeping with the trends in V=O bond lengths (Table 5). The V=O stretching frequency is susceptible to a number of influences, including electron donation from basal plane ligand atoms, solid state effects, and coordination of alkali cations (such as in **3** and $[VO(edt)_2]^{2-}$), so a definitive interpretation of the stretching frequencies is not feasible with the limited data available. Other infrared bands associated with the anions in **1**, **2**, and **3** are ν(C−O)[42] 1272 (**1**), 1266 (**2**), and 1265 cm^{-1} (**3**) and ν(C−C ring stretch)[28] 1446 (**1**), 1457 (**2**), and 1456 cm^{-1} (**3**).

The UV−vis spectra of the tris-complex, **1**, and the vanadyl bis-complex, **3**, are shown in Figure 5, and relevant data for **1**, **2**, and **3** are listed in Table 6 together with data for related compounds. No optical data have been reported for $[V(mp)_3NaLL']_2^{2-}$, which is described as dark brown.[14] **1** and **2** produce dark blue solutions in MeCN, the intense color of which is reflected in the high molar extinction coefficients of the four bands in the visible region. The pattern of these bands is quite similar to that of $(Et_3NH)_2[V(cat)_3]$ in MeCN.[26a] The transitions in **1** and **2** are most reasonably assigned as ligand-to-metal charge transfer. In **2** the bands are slightly red shifted relative to **1**, presumably a consequence of the electron-releasing methyl substituent on the ligands in **2**. **1** is also soluble in water, and the aqueous solution is stable in the absence of air, giving the same color and characteristic UV−vis spectrum as those seen in MeCN solution.

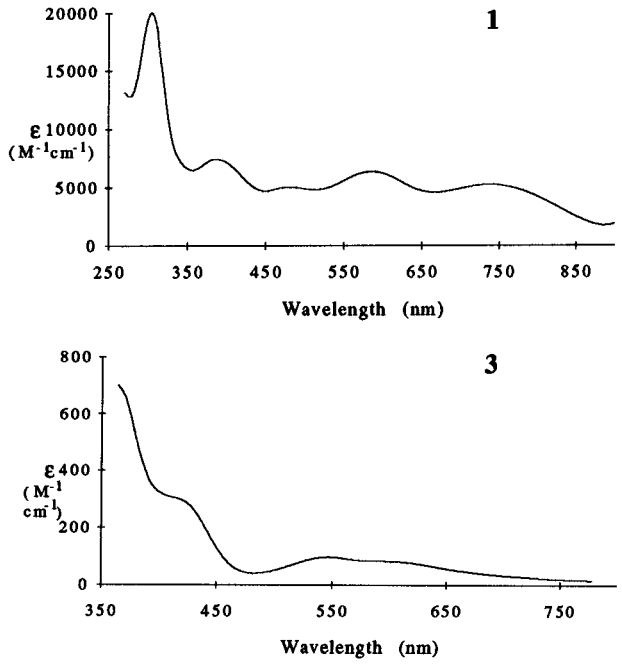

Figure 5. UV−vis spectra of $(Et_3NH)_2[V(mp)_3]$ (**1**) and $Na(Ph_4P)$-$[VO(mp)_2]$ (**3**) in MeCN solution.

Solutions of the vanadyl complex, **3** (MeCN solvent), are considerably lighter in color than those of **1** and **2** and are green,

(41) (a) Selbin, J. *Chem. Rev.* **1965**, *65*, 153−175. (b) Selbin, J. *Coord. Chem. Rev.* **1966**, *1*, 293−314.
(42) Wicklund, P. A.; Brown, D. G. *Inorg. Chem.* **1976**, *15*, 396−400.

Table 7. EPR Parameters of Tris Vanadium(IV) Complexes[a]

complex	donor set	g_0	A_0, 10^4 cm^{-1}	solvent	ref
2 $[V(mmp)_3]^{2-}$	$V(OS)_3$	1.964	71	MeCN	this work
$[V(mp)_3Na(MeCN)(MeOH)]_2^{2-}$	$V(OS)_3$	1.970	70[b]	MeCN	48
$[V(cat)_3]^{2-}$	$V(OO)_3$	1.958	75	MeCN	26
$[V(mnt)_3]^{2-}$	$V(SS)_3$	1.980	58	$CHCl_3$/DMF	30b
$[V(S_2C_6H_3CH_3)_3]^{2-}$	$V(SS)_3$	1.978	62[b]	CH_2Cl_2	47
V(sal-NSO)$_2$	$V(NSO)_2$			DMF	27

complex	g_z	g_x	g_y	A_z, 10^4 cm^{-1}	A_x, 10^4 cm^{-1}	A_y, 10^4 cm^{-1}
2 $[V(mmp)_3]^{2-}$	2.002	1.9802	1.9582	17	75	115
$[V(mp)_3Na(MeCN)(MeOH)]_2^{2-}$	1.952	1.950	1.948	98[b]	98[b]	98[b]
$[V(cat)_3]^{2-}$	1.991	1.937	1.937	14	107	107
$[V(mnt)_3]^{2-}$ [c]	2.000	1.974	1.974	9	91	91
V(sal-NSO)$_2$	1.962	~1.99	~1.99	124	~55	~55

[a] g_0 and A_0 at ambient temperature in solution; g_z, g_x, g_y; A_z, A_x, A_y (absolute values) in frozen solution. [b] Units converted from the published value in *G* by multiplying by $g_e\beta$. [c] Doped in single crystals of $Mo(mnt)_3^{2-}$.

rather than blue, in keeping with what has been observed with the vanadyl bis(catecholates) and vanadium(IV) tris(catecholates).[26,43] The spectrum of **3** is typical of oxovanadium(IV) complexes[41] in displaying three d−d transitions in the visible region and intense charge-transfer transitions in the UV. The two overlapping bands at ca. 600 nm (sh, $\epsilon = 78$ M^{-1} cm^{-1}) and ca. 550 nm ($\epsilon = 92$ M^{-1} cm^{-1}) can be assigned (retaining the C_{4v} symmetry labels of the Ballhausen and Gray MO description[44]) to transitions $b_2(d_{xy}) \rightarrow e(d_{xz},d_{yz})$ and $b_2(d_{xy}) \rightarrow b_1(d_{x^2-y^2})$ respectively, while the third band at ca. 410 nm ($\epsilon \approx 300$ M^{-1} cm^{-1}, a shoulder on the tail of a UV transition) can be assigned to a $b_2(d_{xy}) \rightarrow a_1(d_{z^2})$ transition. Other oxovanadium(IV) complexes with a S_2O_2 ligand set, such as VO(PTO)$_2$[45] (PTO = 2-mercaptopyridine *N*-oxide) and $[VO(maa)_2]^{2-}$ [11] (maa = mercaptoacetic acid), display similar spectra (Table 6).

Magnetic and EPR Measurements. The room temperature magnetic moments of solids **1**, **2**, and **3** are 1.88 (±0.03), 1.83 (±0.03), and 1.68 (±0.03) μ_B, respectively. These results are consistent with the formulation of the complexes as vanadium(IV), d^1 species (μ_{eff} (spin only) = 1.73 μ_B). The room temperature magnetic moment of 1.95 μ_B per vanadium reported[14] for dimeric $(Ph_4P)_2[NaV(mp)_3(MeCN)(MeOH)]_2$ is significantly higher than that of **1** or **2**, but well below what would be expected for a vanadium(III) complex (d^2; μ_{eff} (spin only) = 2.83 μ_B).

In MeCN solution at ambient temperature, intense EPR spectra are observed for **2** and **3**. These spectra are shown in Figure 6 and display the typical eight-line pattern of vanadium (^{51}V; $I = {}^7/_2$), with isotropic g_0 values and hyperfine coupling parameters A_0 given in Tables 7 and 8. The anisotropic frozen solution spectra of **2** and **3** are also shown in Figure 6 and corresponding *g* and *A* values given in Tables 7 and 8, together with EPR data for complexes with related donor sets.

Six-coordinate vanadium(IV) complexes have been shown[46] from previous EPR studies to fall into two groups; those with a $d_{x^2-y^2}$ ground state which display all $g < 2$ and large A_z, and those with a d_{z^2} ground state which display $g_z \approx 2$, g_x, $g_y < 2$ and $A_z \ll A_x$, A_y. The latter parameters can be associated[29] with geometry that is distorted from octahedral toward trigonal prismatic. The EPR parameters for $[V(mmp)_3]^{2-}$ (**2**) (Table 7) clearly place it into this latter category with a d_{z^2} ground state. The isotropic *g* and *A* values for **2** fall between those of $[V(S_2C_6H_3CH_3)_3]^{2-}$ [47] and $[V(O_2C_6H_4)_3]$,[2−] [26] which contain the

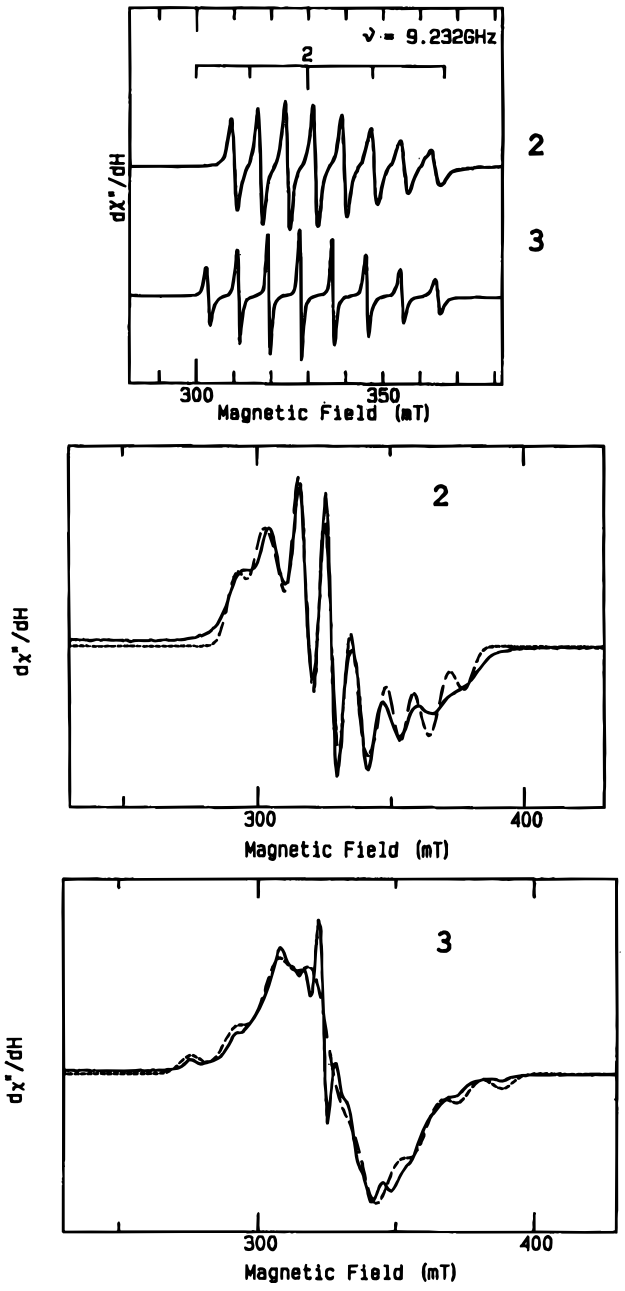

Figure 6. EPR spectra of **2** and **3** in MeCN solution at ambient temperature (upper two plots) and frozen MeCN solution (lower two plots). Computer fitting of frozen solution spectra are shown as dashed lines. The small amount of paramagnetic impurity at $g = 2.02$ in frozen solution spectrum of **3** is ignored in fitting.

(43) Dewey, T. M.; Du Bois, J.; Raymond, K. N. *Inorg. Chem.* **1993**, *32*, 1729−1738.
(44) Ballhausen, C. J.; Gray, H. B. *Inorg. Chem.* **1962**, *1*, 111.
(45) Hodge, A.; Nordquest, K.; Blinn, E. L. *Inorg. Chim. Acta* **1972**, *6*, 491.
(46) Jezierski, A.; Raynor, J. B. *J. Chem. Soc., Dalton Trans.*, **1981**, 1.

Table 8. EPR Parameters of Oxovanadium(IV) Complexes[a]

complex	donor set	g_0	A_0	solvent	ref
3 $[VO(mp)_2]^{2-}$	$VO(OS)_2$	1.985	81	MeCN	this work
$[VO(maa)_2]^{2-}$	$VO(OS)_2$	1.976	81	H_2O	11
$[VO(cat)_2]^{2-}$	$VO(OO)_2$	1.977	82	H_2O	26
$[VO(mnt)_2]^{2-}$	$VO(SS)_2$	1.984	72	$CHCl_3$	30c
$[VO(edt)_2]^{2-}$	$VO(SS)_2$	1.981	72	DMF	40b
VO(tsalen)	$VO(N_2S_2)$			DMF	27

complex	g_z	g_x	g_y	A_z, 10^4 cm^{-1}	A_x, 10^4 cm^{-1}	A_y, 10^4 cm^{-1}
3 $[VO(mp)_2]^{2-}$	1.975	2.007	1.999	150	40	40
$[VO(cat)_2]^{2-}$	1.947	1.981	1.981	154	50	50
$[VO(mnt)_2]^{2-}$ [b]	1.973	1.986	1.986	135	43	43
$[VO(edt)_2]^{2-}$	1.976	1.978	1.977	134	40	40
VO(tsalen)	1.978	1.986	1.986	148	51	51

[a] g_0 and A_0 at ambient temperature in solution; g_z, g_x, g_y; A_z, A_x, A_y (absolute values) in frozen solution. [b] 1:1 CH_2Cl_2/DMF solvent.

dithiolene and catecholate ligands most closely analogous to mmp^{2-}. The g_z , $\langle g_x, g_y\rangle$ and A_z , $\langle A_x, A_y\rangle$ values for **2** are very close to those of the dithiolene $[V(mnt)_3]^{2-}$. Ambient temperature MeCN solution EPR spectra of **2** and $(Ph_4P)_2[V(mp)_3Na(MeCN)(MeOH)]_2$[48] are very similar (Table 7). Thus the room temperature solution magnetic properties of $[V(mp)_3Na(MeCN)(MeOH)]_2^{2-}$ are closer to those of $[V(mmp)_3]^{2-}$ than the room temperature solid state magnetic moments of $(Ph_4P)_2[V(mp)_3Na(MeCN)(MeOH)]_2$ are to $(Et_3NH)_2[V(mp)_3]$ (**1**) or $(Et_3NH)(PNP)[V(mmp)_3]$ (**2**), indicating that $[V(mp)_3Na(MeCN)(MeOH)]_2^{2-}$ may dissociate into monomeric $[V(mp)_3]^{2-}$ units in solution, as proposed[14] by Kang et al., on the basis of structural and electrochemical data. However, in frozen MeCN solution, **2** and $[V(mp)_3Na(MeCN)(MeOH)]_2^{2-}$ differ in that $[V(mp)_3Na(MeCN)(MeOH)]_2^{2-}$ displays an almost isotropic spectrum ($g_z \approx g_x \approx g_y$; $A_z = A_x = A_y$) while that of **2** is distinctly rhombic ($g_z \neq g_x \neq g_y$; $A_z \neq A_x \neq A_y$). This suggests that magnetic interactions between $[V(mp)_3]^{2-}$ units may persist in the solution of $[V(mp)_3Na(MeCN)(MeOH)]_2^{2-}$.

The EPR spectrum of **3** differs from that of **2**, and the *g* and *A* values are typical of the axially symmetric spectra displayed by square pyramidal oxovanadium(IV) complexes with the unpaired electron in an orbital of mostly d_{xy} character (ligands along *x* and *y*).[26b] As can be seen in Table 8, such complexes have $g_z < g_{x,y}$ and $A_z > A_{x,y}$. The d_{xy} ground state is consistent with the electronic spectrum of **3**. Complex **3** is the first well-characterized vanadyl(IV) complex with mixed O,S donors for which EPR data is available. In both **2** and **3** the relation of the hyperfine coupling constants to the analogous catecholates and dithiolenes suggests that the mercaptophenolate ligand is between the catecholate and dithiolene ligands in its ability to delocalize unpaired electron density away from the metal center.

Cyclic Voltammetry. The cyclic voltammogram of **2** in MeCN solution (Figure 7) shows a reversible one-electron process at $E_{1/2} = -0.27$ V (*vs* Ag/AgCl) as well as irreversible processes, one a reduction at -1.08 V and a group of oxidations at $+0.59$, $+0.81$, and $+1.49$ V.

The reversible wave is assigned as an oxidation (i.e. the $V(mmp)_3^{2-}/V(mmp)_3^{-}$ couple) on the basis of: (i) the resting potential found by the instrument is located to more negative potential than the reversible wave; (ii) chemical oxidation of **2** with I_2 or Cp_2Fe^+ ($E_0 \approx 0.4-0.6$ V) in MeCN produces a material, **4**, the cyclic voltammogram of which displays the same features as **2**, but with the resting potential to the positive side of the reversible wave; **4** is therefore identified as the one-electron oxidation product $V(mmp)_3^{-}$; (iii) the UV−vis spectrum (Figure 8) of oxidation product **4** strongly resembles that of **2**, with small but distinct shifts in the positions and intensities of the bands, and the color of **4** is deep emerald green as opposed to the dark blue of **2**; (iv) treatment of MeCN solutions of **4** with oxalate ion ($E_0 \approx -0.5$ V) as reducing agent regenerates the UV−vis spectrum (and color) of **2**.

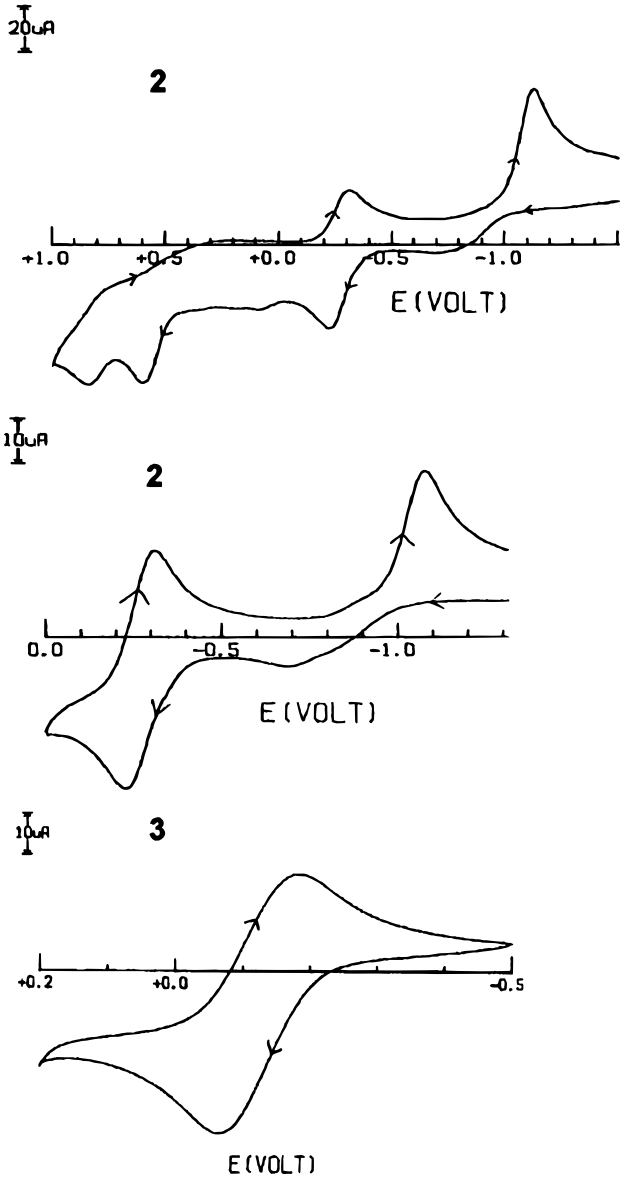

Figure 7. Cyclic voltammograms of **2** and **3** in MeCN solution at room temperature (scan speed 100 mV/s; reference electrode Ag/AgCl).

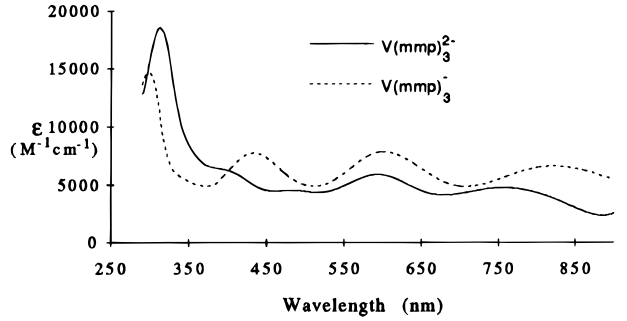

Figure 8. UV−vis spectra of $(Et_3NH)(PNP)[V(mmp)_3]$ (**2**) and $(Et_3NH)[V(mmp)_3]$ (**4**) in MeCN solution.

(47) Davison, A.; Edelstein, N.; Holm, R. H.; Maki, A. H. *Inorg. Chem.* **1965**, *4*, 55.
(48) Weng, L.; Liu, H.; Sun, Q.; Huang, X.; Kang, B. *Bopuxue Zazhi* **1991**, *8*, 365−370.

The chemically reversible interconversion between **2** and **4** is represented in eq 3.

$$\underset{\mathbf{2}}{[V(mmp)_3]^{2-}} \underset{\text{oxalate}}{\overset{I_2 \text{ or } Cp_2Fe^+}{\rightleftharpoons}} \underset{\mathbf{4}}{[V(mmp)]_3^-}$$

Solutions of **2** (in MeCN) exposed to the air for several minutes develop the color and UV−vis spectrum of **4**. Prolonged exposure to air leads to complete decolorization of the solution and loss of the visible spectrum.

The irreversible reduction at −1.08 V is for the process $V(mmp)_3^{2-} \rightarrow V(mmp)_3^{3-}$ and the irreversible oxidations at +0.59, +0.81, and +1.49 V are probably ligand-based processes.

The electrochemical behavior of **1** is entirely analogous to that of **2**, with small shifts observed in the cyclic voltammetry consistent with the slight electron-donating effect of the methyl group in **2**. The reversible changes in the UV−vis spectrum of **1** upon oxidation to $V(mp)_3^-$ and subsequent reduction back to **1** also closely parallel those described above for **2** ⇄ **4**. The cyclic voltammogram reported for $[V(mp)_3Na(MeCN)(MeOH)]_2^{2-}$ in DMF[14] is similar to that of **1** and **2**, but the reversible wave ($E_{1/2}$ = −0.28 V, *vs* Ag/AgCl) is described as referring to the $V(mp)_3^{2-} \rightleftarrows V(mp)_3^{3-}$ process.

The cyclic voltammogram of **3** displays a quasi-reversible process centered at −0.12 V (*vs* Ag/AgCl). Since reductions of related oxovanadium(IV) complexes with sulfur donors (such as $VO(PTO)_2$[49] and VO(tsalen)[27]) occur at potentials more negative than −1 V, the wave is reasonably assigned as an oxidation. The position of the resting potential is consistent with this assignment. Vanadyl(IV) dithiolenes $[VO(mnt)_2]^{2-}$ and $[VO(S_2C_6Cl_4)]^{2-}$ display reversible oxidations at +0.42 and +0.13 V, respectively, assigned as the 2−/1− couples.[50] Quasi-reversible oxidation waves at potentials ranging from +0.05 to −0.10 V were reported for some vanadyl(IV) catecholates,[43] and these have been associated with metal-centered V(V)/V(IV) couples. These catecholates also display irreversible oxidations at +0.67 V from oxidation of the ligand. Irreversible oxidation waves for **3** are found at +0.63, +0.97, and +1.43 V (these waves disappear on repeated scanning) and are also probably ligand-based processes.

Compounds **1**, **2**, and **3** contain an early transition metal in a relatively high oxidation state combined with a ligand that presents both hard and soft Lewis base donor atoms. Furthermore, the ligand is potentially redox active, and oxidation or reduction products of the complexes could display varying degrees of quinone or thione ligand forms:

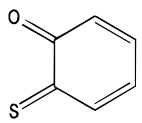

quinone/thione

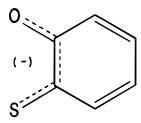

semi-quinone/thione

Oxidation of the ligand to the disulfide $^-OC_6H_4SSC_6H_4O^-$, which can coordinate as a tridentate ligand, has been observed,[51] but evidence for quinone/thione forms has not been reported and could be provided by structural comparison between species related by the addition or removal of one or more electrons, such as $[V(mp)_3]^{2-}$ and $[V(mp)_3]^-$. The combination of Lewis acid and Lewis base sites in suitable steric juxtaposition has been shown[52] to be applicable to the activation of small molecules, such as CO_2. In **1**, **2**, and **3** the oxophilic Lewis acid vanadium(IV) and the nucleophilic S of the ligand can potentially act in concert in such activation reactions. We are investigating the reactivity of **1**, **2**, and **3**, as well as pursuing the structural characterization of the oxidation products of **1** and **2**.[53]

Acknowledgment. This research was supported by a William and Flora Hewlett Foundation Award of Research Corporation. We acknowledge and thank Dr. William R. Dunham, Professor Fred L. Urbach, and Shawn Swavey for EPR measurements and Kostas Demadis for electrochemical measurements. We also thank Professor Dimitri Coucouvanis for his interest and advice.

Supporting Information Available: Listings of crystal data and structure refinement parameters, atomic coordinates and equivalent isotropic displacement parameters, all bond lengths and angles and selected torsion angles and least-squares planes, anisotropic displacement parameters, and hydrogen coordinates and isotropic displacement parameters and structural diagrams of the PNP cation in **2**, the Ph_4P cation in **3**, and the ether coordinated to Na in **3** (35 pages). Ordering information is given on any current masthead page.

IC950792B

(49) Shim, Y. B.; Choi, S. N. *Bull. Korean Chem. Soc.* **1987**, *8*, 225−230.
(50) McCleverty, J. A.; Locke, J.; Ratcliff, B.; Wharton, E. J. *Inorg. Chim. Acta* **1969**, *3*, 283−286.
(51) (a) Roberts, S. A.; Darsey, G. P.; Cleland, W. E., Jr.; Enemark, J. H. *Inorg. Chim. Acta* **1988**, *154*, 95. (b) Chen, X. T.; Liu, H. Q.; Kang, B. S.; Weng, L. H.; Huang, L. R.; Wu, D. X.; Lei, X. J. *J. Coord. Chem.* **1990**, *22*, 109.
(52) For example: Fachinetti, G.; Floriani, C.; Zanazzi, P. F. *J. Am. Chem. Soc.* **1978**, *100*, 7405.
(53) We have prepared the niobium(V) analogues of **1** and **2**. The structure and properties of $[Nb(mmp)_3]^-$ will be reported elsewhere.